Journal of Engineering and Applied Sciences 13 (Special Issue 8): 6316-6323, 2018
ISSN: 1816-949X

Instantaneous Reactive Power Theorem (IRPT) Based Control of Doubly Fed Induction Generator (DFIG) Connected to Variable Speed Wind Turbine

Ghorakavi Deepthi, Anjana Jain and S. Shankar
Department of Electrical and Electronics Engineering, Amrita School of Engineering,
Amrita University, Bengaluru, Amrita, Vishwavidyapeetham, India

Abstract: This research includes study of Doubly Fed Induction Generator (DFIG) connected to variable speed Wind Energy Conversion System (WECS). WECS connected to grid is composed of back-to-back PWM converters on the rotor side. Instantaneous Reactive Power Theorem (IRPT) based control technique is used for Rotor Side Converter (RSC) control and Direct Power Control (DPC) is used for Grid Side Converter (GSC) control. Proposed control strategy is used for voltage and frequency control of DFIG. IRPT helps in reactive power compensation, attaining unity power factor and reduction of harmonics. The developed system is validated using MATLAB/Simulink for different dynamic conditions.

Key words: DFIG, RSC control, GSC control, IRPT control, DPC, MATLAB

INTRODUCTION

From past few decades, Wind Power Plants (WPPs) are fast growing alternative energy source. In the initial days, Squirrel Cage Induction Generator (SCIG) was used to connect to the grid but recently most of the WPPs are using DFIG rather than SCIG, due to its capacity to work atvariable speed which increases the efficiency of the system. Maximum Power Point Tracking (MPPT) in variable speed WECS is used to realize maximum efficiency as well as energy extraction from the system. One of the popular methods of MPPT is obtaining maximum efficiency through the characteristic power curve which is accomplished on a turbine-rotor nonlinear mechanical system with the help of small signal stability analysis (Zou *et al*., 2011). The WECS connected to grid can be applicable in hybrid Remote Area Power Supply (RAPS) systems which provides control of frequency and voltage improvement by the accomplishment of MPPT (Mendis *et al*., 2012). MPPT is also used for power smoothening in a grid connected DFIG for variable speed WECS (Naidu and Singh, 2017; Sleiman *et al*., 2013). Rotor side control of DFIG is used to achieve unity power factor at the stator terminals and MPPT whereas grid side control is used to supply regulated power to the grid. BESS is used in order to maintain regulated power at the grid even though if there is any change in wind speed. The other method of controlling DFIG is decoupled control of reactive and active power in which the GSC controller is used to achieve DC link voltage and power factor at rotor terminals using conventional P-I controllers (Pati and Samantray, 2014). To achieve constant active power for variations in wind conditions a storage unit is incorporated in the WECS (Djeriri *et al*., 2014). The battery or any device that store energy incorporation in DC link facilitates storage of energy temporarily. For the adjustment of power factor on the source side under equitable load condition reactive power control strategy is used (Win *et al*., 2015; Chen and Chen, 2014). Direct voltage control is also one of the control strategies for the control of DFIG (Jain, 2015). The disproportions in wind energy resentfully effect the conversion in energy which can be minimized by using DFIG. Direct power control is another control strategy to maintain stator terminal frequency and voltage at the same time to maintain DC link voltage of the grid interconnected WECS (Jain *et al*., 2016). WECS based DFIG possess many benefits like more efficiency, power factor correction is easy, flexible operation for variable speed which lead to energy produced is 20-30% higher, four quadrant operation of active and reactive power, reduced converter cost (Sivakumar *et al*., 2017; Subramanian *et al*., 2011). IRPT helps in power quality improvement which leads to many advantages like attaining unity power factor, reactive power control, achieving maximum efficiency and so on (Bangarraju *et al*., 2014). The DFIG concept is greatly attractive and in general, the windings of the stator are directly connected to the grid whereas the rotor winding employs bidirectional PWM Voltage Source Converters (VSC) along with dc link.

Corresponding Author: Ghorakavi Deepthi, Department of Electrical and Electronics Engineering, Amrita School of Engineering, Amrita University, Bengaluru, Amrita Vishwavidyapeetham, India

MATERIALS AND METHODS

WECS

Wind turbine: The burning of fossil fuels adversely affects the global climate. Hence, the source of electricity generation, in addition to measures of demand side which is cost effective and low carbon has become essential. So, wind energy has become one of the fastest growing energy industries. According to principle of energy-mass conservation in wind, the maximum power that can be extracted from wind is given as:

$$P_{wind} = \frac{1}{2} \rho A V_w^3 \quad (1)$$

Where:
Cp = Maximum Power Coefficient
V_w = Wind Velocity
P = Density of air
A = Swept area

The power coefficient of the wind turbine is defined as the ratio of turbine power to the maximum power that can be extracted from wind:

$$C_p = \frac{\text{Turbine power}(p_{turbine})}{\text{Power obtained from wind}(p_{wind})}$$

Hence, the power extracted from the turbine is given by:

$$P_{turbine} = p_{wind}\, C_p = \frac{1}{2} \rho A V_w^3\, C_p \quad (2)$$

Dynamic characteristics of wind turbine: The power from wind turbine for transients in wind variation is given by:

$$P_{turbine} = p_{wind}\, C_p = \frac{1}{2} \rho A V_w^3\, C_p(\lambda,\beta) \quad (3)$$

$$C_p(\lambda,\beta) = C_1\left(\frac{C_2}{\lambda_i} - C_3\beta - C_4\right) e^{\frac{-C_5}{\lambda_i}} + C_6\beta \quad (4)$$

Where:

$$\lambda_i = \left(\frac{1}{\lambda + 0.008\beta} - \frac{0.035}{\beta^3 + 1}\right) \quad (5)$$

where, • is the tip speed ratio of the turbine:

$$\lambda = \frac{\text{Rotational speed of rotor}(w_r) * \text{radius}(r)}{(\text{Wind velocity}(v)_w)} \quad (6)$$

Figure 1 shows the dynamic characteristics of maximum power extracted from wind turbine with respect to change in turbine speed for different wind velocities.

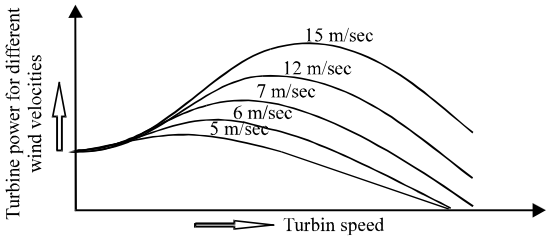

Fig. 1: Characteristics of power extracted from turbine with respect to turbine speed for different wind velocities

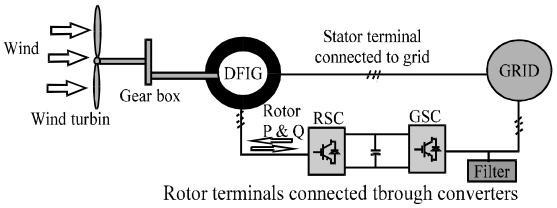

Fig. 2: Block diagram of WECS which employ DFIG

DFIG: Variable speed WECS produces high energy; Possess pitch control, less mechanical loads, reduction in noise and variation in power output, control of active power and reactive power. One of the machines that employ variable speed principle is DFIG. Its power delivery to the grid is carried out through stator which is directly connected to the grid and rotor (connected to the grid through back to back PWM converters). Advantages of DFIG are the ability to control reactive power, less converter losses (only small amount of total power has to be handled by the converters). DFIG optimizes turbine for lower wind velocities whereas during higher wind velocities reduction in mechanical losses is obtained leading to extraction of maximum energy from the total energy available in the wind, hence, efficiency of the system is improved and power factor is controlled. Figure 2 represents the basic block diagram of DFIG. DFIG can work in three modes (sub-synchronous, super-synchronous and synchronous) depending on the wind velocity variations. In sub-synchronous mode of operation the rotor will take power from the grid whereas in super-synchronous mode of operation it gives power to the grid through bidirectional converters. Hence, the slip power of the machine can flow in two directions. Power during super-synchronous mode of operation is given by:

$$P_m = (1+s)p_{rotor} \quad (7)$$

where, s is defined as the slip. Power during sub-synchronous mode of operation is given by:

$$P_m = (1-s)p_{rotor} \quad (8)$$

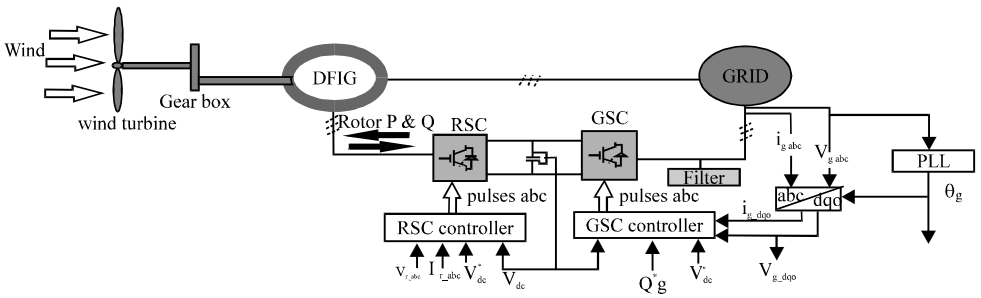

Fig. 3: Control of DFIG with GSC and RSC controllers

Control technique: In the proposed control strategy, RSC is used to control the stator terminal frequency and voltage and active and reactive powers at the stator terminals are maintained. The GSC controls the DC link voltage which is used to maintain the voltage and frequency as well as reactive power at the rotor terminals. DC link capacitor is used to reduce fluctuations in the DC link voltage. The proposed control strategy uses IRPT control technique for RSC controller and DPC (Vector) control technique for GSC to control the system depicted in Fig. 3.

GSC controller: The two main objectives of proposed control strategy for GSC controller are; To maintain DC link voltage constant and control reactive power that is been exchanged between rotor and grid. Therefore, the voltage vector of grid is aligned with synchronous reference frame direct axis and indirect axis component is maintained null. The required equations for GSC control are given by:

$$v_{fd} = -\left(R_f idg + L_f \frac{di_{dg}}{dt}\right) + v_{sd} + w_s L_f i_{qg} \quad (9)$$

$$v_{fq} = -\left(R_f i_{qg} + L_f \frac{di_{qg}}{dt}\right) - w_s L_f i_{dg} \quad (10)$$

$$p_g = \frac{3}{2}\left(v_{sd} i_{dg} + v_{sq} i_{qg}\right) = \frac{3}{2} v_{sd} i_{dg} \quad (11)$$

$$Q_g = \frac{3}{2}\left(v_{sd} i_{dg} + v_{sq} i_{qg}\right) = -\frac{3}{2} v_{sd} i_{qg} \quad (12)$$

Where:

v_{fd} and v_{fq} = Vector output voltage components of GSC

i_{dg}, i_{qg} and v_{sd} = Current and voltage components of grid, respectively where as $v_{sq} = 0$ (Fig. 4)

According to Slip (s) sign, through rotor active power of DFIG is interchanged with grid. Equation 11 and

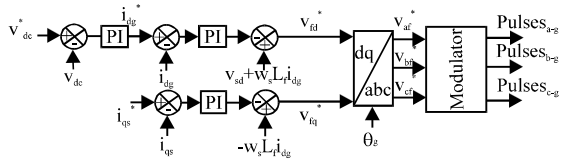

Fig. 4: GSC Controller for DFIG

12 states that DC link voltage and Active power can be controlled with the help of whereas the flow of reactive power in the grid can be controlled with the help of . The design of controllers follows the same from as shown in Eq. 13 and 14:

$$v^*_{fd} = -k_{pi}\Delta i_{dg} - kii\int \Delta i_{dg} dt + \left(v_{sd} + w_s L_f i_{qg}\right) \quad (13)$$

$$v^*_{fd} = -k_{pi}\Delta i_{qg} - kii\int \Delta i_{qg} dt - w_s L_f i_{dg} \quad (14)$$

where, • $i_{dg} = I^*_{dg} - i_{dg}$ and • $i_{qg} = I^*_{qg} - i_{qg}$. The proportional and integral constants of the current loop are k_{pt} and k_{ii} respectively. The controller integral time constant is given by $T_{ii} = k_{pt} \backslash k_{ii}$ Stability and transient response can be maintained properly by detecting angular position of grid voltage which is measured using Phase Locked Loop (PLL) (Sleiman *et al*., 2013). For transforming three phase system variables to dq0 reference frame the locked angle is used. Outer PI controller is used to DC link voltage constant though there is change in wind speed which leads to change in the generator speed. This PI controller carries the error that is the difference between the measured and reference DC link voltages and generate i^*_{dg}. i^*_{qg} is kept at zero in order to compensate for reactive component of power at grid side. Magnetizing energy required is also provided GSC through DFIG rotor. Compare the measured and reference grid currents and then process through the inner current PI controllers to generate pulses for GSC.

RSC controller: IRPT control technique is used for RSC controller which is sworn to control DIF in order to extract maximum mechanical power from wind turbine

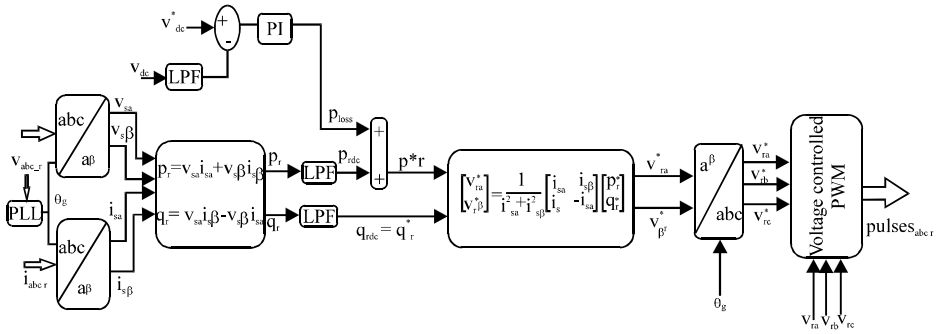

Fig. 5: RSC controller algorithm

and also to attain unity power factor at the terminals of stator. In the proposed control technique the stator resistance is neglected and an assumption is made that the grid is under balanced voltage condition, the magnetic flux of the stator is maintained constant and is imposed by grid. Voltage vector of the stator is aligned with direct axis. The inputs to the RSC controller are the three phase voltage and current obtained at the rotor terminals. Using Clark's transformation the three phase components are transformed to •-• frame. The transformed •-• components of rotor voltages and currents are used to calculate instantaneous active power and reactive power. These powers consists of ac as well as dc components and are given by:

$$pr = v_{sa}i_{sa} + v_{sb}i_{sb} + v_{sc}i_{sc} + = v_{sa}i_{sa} + v_{s\beta}i_{s\beta} + = p_{rdc}p_{rac} \quad (15)$$

$$Qr = \frac{1}{\sqrt{3}}\left(i_{sa}\left(v_{sa}-v_{sb}\right)+i_{sb}\left(v_{sb}-v_{sc}\right)+i_{sc}\left(v_{sa}-v_{sa}\right)\right) = \quad (16)$$
$$v_{sa}i_{s\beta}-v_{sa\beta}i_{sa} = q_{rdc}+q_{rac}$$

To extract dc component from the instantaneous active and reactive power low pass filter is used. A PI Controller is used to maintain DC bus voltage of RSC. The design of PI controller follows the Eq. 19

$$p_{loss(k)} = p_{loss(k-1)} + k_p\left(v_{dc(k)}-v_{dc(k-1)}\right)+k_q v_{dc(k)} \quad (17)$$

Where k_p and k_q are the proportional and integral gains of DC bus voltage. The obtained $p_{loss(k)}$ is the power loss active component of RSC. Reference component of active power p^*_r is obtained by adding p_{loss} to dc component of the active power and is represented as:

$$p^*_r = p_{rdc} + p_{loss} \quad (18)$$

Reference component of the reactive power is the DC component of the reactive which is obtained after passing the reactive power of the rotor through low pass filter. The reference component is given by:

$$q^*_r = q_{rde} \quad (19)$$

Using the reference components of the active power and reactive power the reference rotor voltages in •-• frame are generated using the equations given in Eq. 22. Equations in •-• frame are transformed to three phase reference a-c system using Clark's transformation. The equations of transformation are given by:

$$\begin{bmatrix} v^*_{r\alpha} \\ v^*_{r\beta} \end{bmatrix} = \frac{1}{i^2_{sa}+i^2_{s\beta}}\begin{bmatrix} i_{sa} & i_{s\beta} \\ i_{s\beta} & i_{sa} \end{bmatrix}\begin{bmatrix} p^*_r \\ q^*_r \end{bmatrix} \quad (20)$$

The obtained reference voltages are compared with the measured rotor voltages to obtain gating pulses for RSC. Figure 5 gives the schematicv representation of RSC controller.

The proposed control technique is implemented for different wind velocities on a doubly fed induction generator with the specifications of the machine as mentioned in Appendix A. The entire system is developed using MATLAB/Simulink.

RESULTS AND DISCUSSION

The simulation results of the proposed system are clearly discussed with variable wind velocity and variable loads conditions in sections A-C.

Characteristics of wind turbine: As mentioned in the section 2(B) the wind turbine is designed for the dynamic variations in the wind velocity and the characteristics are obtained as shown in Fig. 6 and 7 which is similar to that of the Fig. 1.

Simulation results with variation in wind velocity: From Fig. 8-10 shows the change in torque and rotor speed with step change in wind velocity from 5-15 m/sec

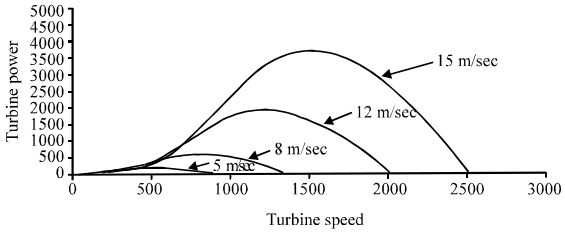

Fig. 6: Characteristics of designed wind turbine

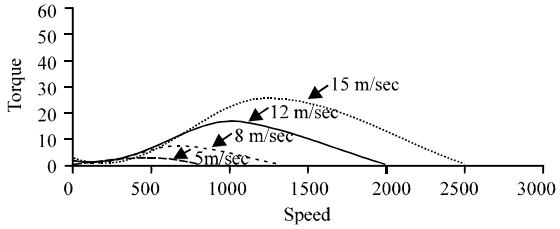

Fig. 7: Torque-speed characteristics of wind turbine

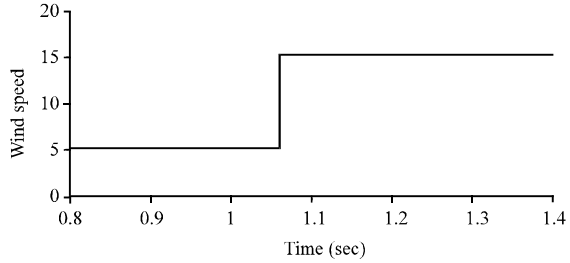

Fig. 8: Variation in wind velocity

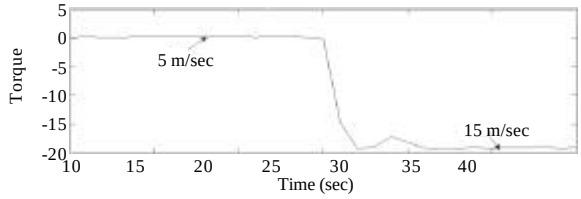

Fig. 9: Variation in torque for different wind velocities

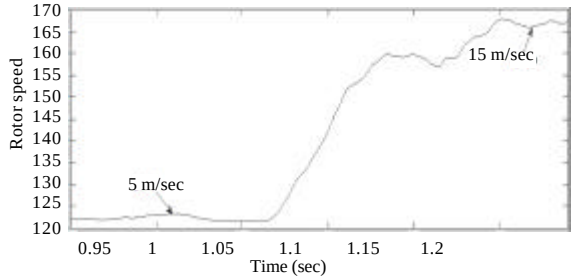

Fig. 10: Variation in rotor speed for variation in wind velocities

15 m/sec. Through RSC stator terminal voltage and frequency is maintained constant, shown in Fig. 11 and 12. Figure 13 shows the flow of stator power to the grid.

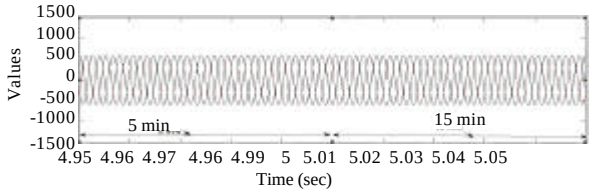

Fig. 11: Stator terminal voltage

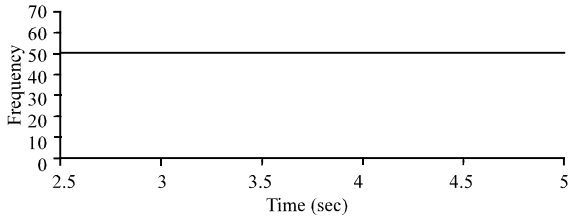

Fig. 12: Stator terminal frequency

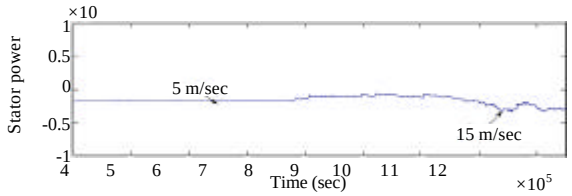

Fig. 13: Power flow between stator and grid

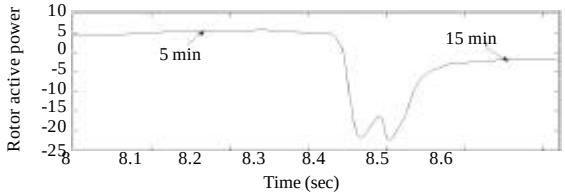

Fig. 14: Rotor active power flow for different wind velocities

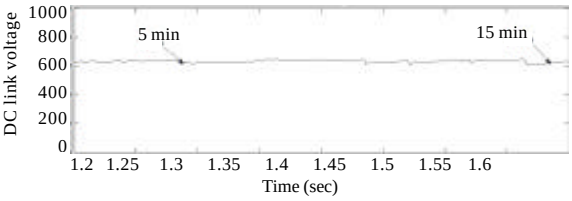

Fig. 15: DC-link voltage for variation in wind velocities

Rotor power flows during sub and super synchronous mode of operation through bidirectional converters is shown in Fig. 14. DC link voltage, voltage and current injected to the grid respectively are shown in Fig. 15-17. In this section the results were shown for variations in the wind velocities while keeping load constant, shown in Fig. 18.

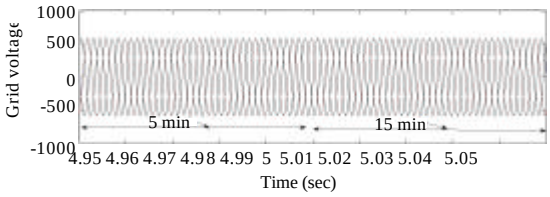

Fig. 16: Voltage injected to grid

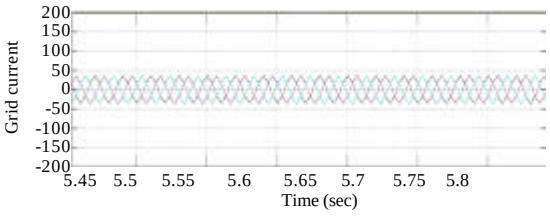

Fig. 17: Current injected to grid

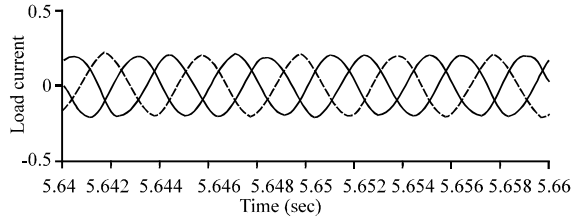

Fig. 18: Load current

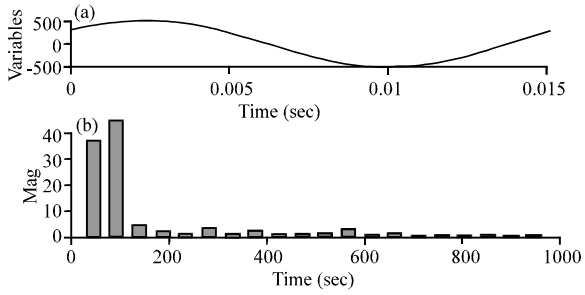

Fig. 19: Total harmonic distortion for voltage, FFT window: 1 of 2500 cycles of selected signal; Fundamental (50 Hz) = 559 , THD = 1. 46%

Simulation results with load variation: This study shows different results wrt to load variation while keeping wind velocity and torque constant. Figure 20 shows variation in the load (current) with constant wind velocity and constant torque (Fig. 21 and 22). When a constant torque is given to the machine the sped of the rotor will also be constant shown in Fig. 23. Figure 24-30 represents stator terminal voltage, stator terminal frequency, power flow between machine and grid, DC bus voltage, voltage and current injected to the grid.

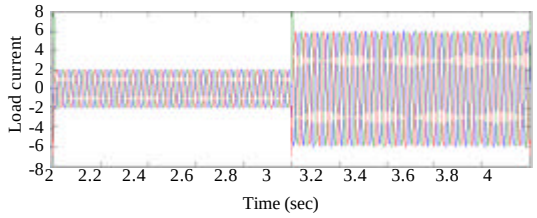

Fig. 20: Variation in load (current)

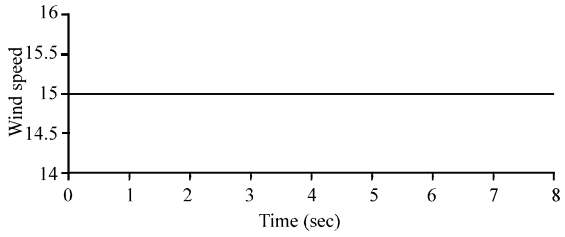

Fig. 21: Wind velocity

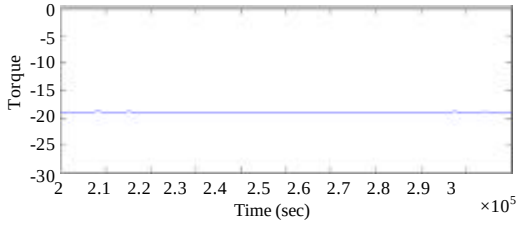

Fig. 22: Torque for different load conditions

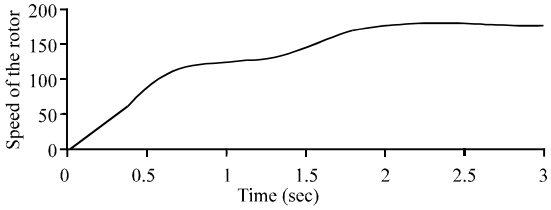

Fig. 23: Speed of machine for different loads

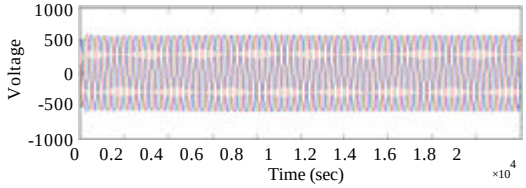

Fig. 24: Stator terminal voltage

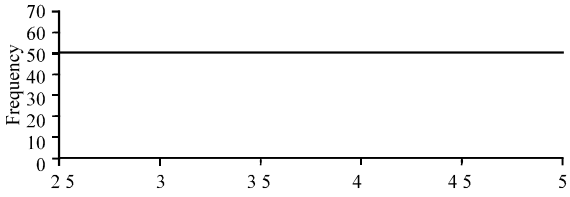

Fig. 25: Stator terminal frequency

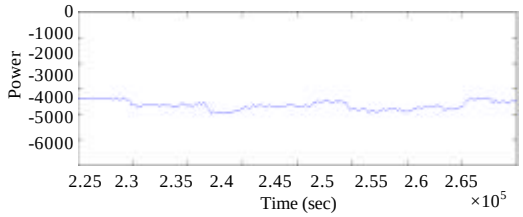

Fig. 26: Power flow between stator and grid

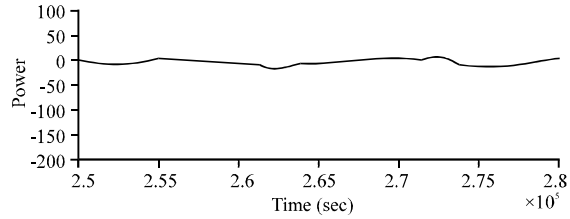

Fig. 27: Power blow between rotor and grid

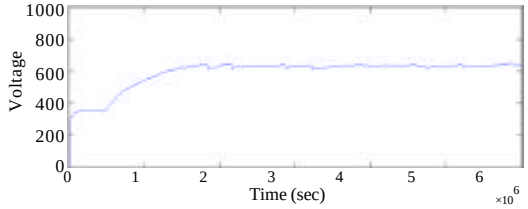

Fig. 28: DC bus voltage

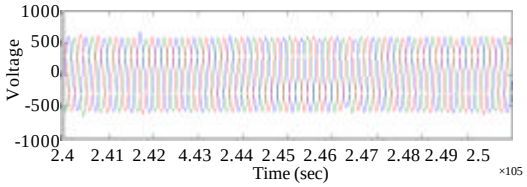

Fig. 29: Voltage injected to grid

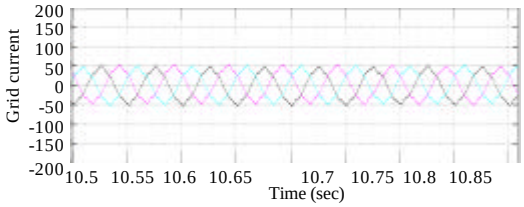

Fig. 30: Current injected to grid

Table 1: Power flow of stator and rotor for variation in wind speed

Wind velocity (m/sec)	Rotor speed (rad/sec)	Stator Power (W)	Rotor power (W)	DC link Voltage (V)
5	120	-1120	5	630
15	165	-3548	-4	630

CONCLUSION

This study has given a new control technique for the control of DFIG connected to a variable speed turbine. The system always feed grid irrespective of the variation in wind speed. The proposed control technique encloses IRPT control algorithm for RSC controller and DPC control technique for GSC controller. By applying this control algorithm the system complexity has reduced and the grid synchronization is maintained properly that is voltage and frequency of the power between grid and machine is maintained and also the active and reactive power. The system is modeled, developed and simulated using MATLAB/Simulink. The power flow of stator and rotor are tabulated in Table. The power quality of the system is also improved.

Appendix A:

- Machine parameters: 5 HP, 50 Hz, 415 V, 4 pole
- Stator resistance = 2.375 •
- Rotor resistance = 3.9416 •
- Stator and rotor inductance = 0.02386 H
- Magnetizing inductance = 0.18134 H
- Rotor inertia = 0.15 kg-m^2
- Friction of coefficient = 0.022

REFERENCES

Bangarraju, J., V. Rajagopal and A. Jayalaxmi, 2014. Implementation of three leg VSC based DVR using IRPT control algorithm. Proceedings of the 2014 IEEE 6th India International Conference on Power Electronics (IICPE), December 8-10, 2014, IEEE, Kurukshetra, India is BN:978-1-4799-6045-3, pp: 1-6.

Chen, H.C. and P.H. Chen, 2014. Active and reactive power control of a doubly fed induction generator. Appl. Math. Inf. Sci., 8: 117-124.

Djeriri, Y., A. Meroufel, A. Massoum and Z. Boudjema, 2014. Direct power control of a doubly fed induction generator based wind energy conversion systems including a storage unit. J. Electr. Eng., 14: 196-204.

Jain, A., 2015. Control of doubly fed induction generator connected to variable speed wind turbine. Proceedings of the 2015 International Conference on Technological Advancements in Power and Energy (TAP Energy), June 24-26, 2015, IEEE, Kollam, India isBN:978-1-4799-8281-3, pp: 500-505.

Jain, A., C.T. Vijay, S. Shravanthi and S. Gokul, 2016. Comparative analysis of Direct Power Control (DPC) and Direct Voltage Control (DVC) for control of Doubly Fed Induction Generator (DFIG) connected to a variable speed wind turbine. Intl. J. Control Theory Appl., 9: 8961-8971.

Mendis, N., K.M. Muttaqi, S. Sayeef and S. Perera, 2012. Standalone operation of wind turbine based variable speed generators with maximum power extraction capability. IEEE. Trans. Energy Conversion, 27: 822-834.

Naidu, N.S. and B. Singh, 2017. Grid-interfaced DFIG-based variable speed wind energy conversion system with power smoothening. IEEE. Trans. Sustainable Energy, 8: 51-58.

Pati, S. and S. Samantray, 2014. Decoupled control of active and reactive power in a DFIG based wind energy conversion system with conventional PI controllers. Proceedings of the International Conference on Circuits, Power and Computing Technologies (ICCPCT-2014), March 20-21, 2014, IEEE, Nagercoil, India isBN:978-1-4799-2405-9, pp: 898-903.

Sivakumar, K., J. Ramprabhakar and S. Shankar, 2016. Coordination of wind-hydro energy conversion system with sliding mode control. Proceedings of the 2016 IEEE 1st International Conference on Power Electronics, Intelligent Control and Energy Systems (ICPEICES), July 4-6, 2016, IEEE, Delhi, India isBN:978-1-4673-8588-6, pp: 1-5.

Sleiman, M., B. Kedjar, A. Hamadi, K. Al-Haddad and H.Y. Kanaan, 2013. Modeling, control and simulation of DFIG for maximum power point tracking. Proceedings of the 9th Asian Control Conference (ASCC), June 23-26, 2013, IEEE istanbul, Turkey is BN:978-1-4673-5767-8, pp: 1-6.

Subramanian, S., J.K. Chatterjee, V. Rajasekhar and A. Kondalarao, 2011. Reduction of grid current harmonic injection in matrix converter controlled induction generator for wind applications. Proceedings of the 2011 International Conference on Power and Energy Systems, December 22-24, 2011, IEEE, Chennai, India isBN:978-1-4577-1508-2, pp: 1-6.

Win, T.S., Y. Hisada, T. Tanaka, E. Hiraki and M. Okamoto *et al*., 2015. Novel simple reactive power control strategy with DC capacitor voltage control for active load balancer in three-phase four-wire distribution systems. IEEE. Trans. Ind. Appl., 51: 4091-4099.

Zou, Y., M. Elbuluk and Y. Sozer, 2011. Stability analysis of Maximum Power Point Tracking (MPPT) method in wind power systems. Proceedings of the Annual Conference on Industry Applications Society (IAS) Vol. 49, October 9-13, 2011, IEEE or lando, Florida, USA. is BN:978-1-4244-9498-9, pp: 1-8.